Microstructure and thermal properties of plasma-sprayed ceramic thermal barrier coatings

Ceramic thermal barrier coatings (TBCs) are advanced systems for more efficient aircraft and gas turbine engines, due to their unique microstructural, thermal and mechanical properties. In this work the microstructural and thermal properties of air-plasma-sprayed zirconia based and lanthanum zirconate ($La_2Zr_2O_7$) coatings were investigated. All the TBCs herein employed exhibited a porous microstructure, composed of thin lamellae embedded in a network of pores and microcracks. Ceria-yttria co-stabilized zirconia (CYSZ) coatings showed the highest thermal expansion coefficient. In turn, $La_2Zr_2O_7$ coatings exhibited the lowest specific heat capacity at room temperature. Unlike CYSZ coatings, the specific heat capacity of yttria stabilized zirconia (YSZ) and lanthanum zirconate coatings increases after heating cycles, due to sintering effects. These investigations have also been addressed to the development of a novel multilayered TBC system, composed of two or more ceramic top coats, where CYSZ is used as an intermediate layer and coated with one or more rare-earth zirconates layers

■ *Giovanni Di Girolamo, Caterina Blasi, Alida Brentari, Monica Schioppa*

Microstruttura e proprietà termiche di barriere termiche ceramiche realizzate mediante plasma spraying

Le barriere termiche ceramiche sono sistemi avanzati per motori aeronautici e turbine a gas, grazie alle loro caratteristiche microstrutturali, termiche e meccaniche. In questo lavoro sono analizzate le proprietà microstrutturali e termiche di rivestimenti a base di zirconia e di zirconato di lantanio, realizzati mediante "plasma spraying". Tutte le barriere termiche presentano una microstruttura lamellare porosa, caratterizzata dalla presenza di pori e microcricche. I rivestimenti in zirconia stabilizzata con ceria ed yttria (CYSZ) presentano il più elevato coefficiente di espansione termica. A loro volta, i rivestimenti in zirconato di lantanio (La2Zr2O7) presentano la più bassa capacità termica a temperatura ambiente. Diversamente dai rivestimenti in CYSZ, la capacità termica dei rivestimenti in zirconia stabilizzata con yttria e in zirconato di lantanio aumenta dopo i cicli di riscaldamento, a causa della sinterizzazione della microstruttura. Queste analisi sono state anche indirizzate allo sviluppo di un sistema a barriera termica innovativo multistrato, costituito da due o più strati ceramici, dove lo strato intermedio realizzato in CYSZ è rivestito da uno o più strati di zirconati di terre rare

Introduction

Thermal barrier coatings are advanced systems for protection of Ni-based super-alloy hot-section parts of turbine engines, such as first-stage blades, stator vanes

■ **Giovanni Di Girolamo, Caterina Blasi, Monica Schioppa**
   ENEA, Technical Unit for Brindisi Material Technologies

■ **Alida Brentari**
   ENEA, Technical Unit for Faenza Material Technologies

and transition pieces[1,2]. They allow to increase the durability of these components, by reducing the temperature on the metal surface and the environmental attack promoted by oxygen, molten salts and particulates during service. In addition, their application allows to significantly increase the engine efficiency as well as to reduce the fuel consumption and the emissions of CO and NO_x in the atmosphere.

A typical TBC system is composed of a metallic bond coat and a ceramic top coat. The bond coat is able to improve the adhesion of the ceramic coating and provides good resistance to high-temperature oxidation and corrosion. In turn, ceramic materials with low thermal conductivity are able to reduce the heat transfer to the underlying metal and to improve the capability, the thermal cycling lifetime and the resistance to the environmental attack from highly corrosive media[3,4,5]. Plasma spraying is a cost-effective deposition technique for manufacturing of porous TBCs. Powder particles are injected into a high-temperature plasma gas jet, melted and accelerated. When impacting on the substrate, they are flattened and quenched, thus forming a coating with a layered microstructure containing pores, splat boundaries and microcracks. The high deposition rate of the plasma spray process involves shorter manufacturing times and lower costs in comparison with electron beam physical vapor deposition (EB-PVD): lower equipment costs and ease of deposition. In addition, more heat resistant TBCs can be manufactured due to their lamellar and porous microstructure.

Partially yttria stabilized zirconia (YSZ) is the state-of-the-art material used for ceramic TBCs, due to its good mechanical and thermal properties. However, at temperature higher than 1200 °C, YSZ TBCs are affected by accelerated sintering and by phase transitions. Sintering promotes the growth of crystallites, so that the pores among grain boundaries are gradually filled, reducing the strain tolerance and the thermal cycling lifetime. In turn, high-temperature exposure at temperatures above 1200 °C produces the partial decomposition of metastable t' zirconia phase and the formation of a high-yttria cubic phase and a low-yttria tetragonal phase which can, in turn, transform to monoclinic phase during cooling. This last transformation typically involves volume change and cracking.

Nevertheless, up to now no composition with better performance than YSZ has been clearly detected. The attention of TBC designers is currently focused on ceramic materials characterized by low thermal conductivity, high phase stability, thermal expansion coefficient (CTE) close to that of metal substrate, high hardness, low Young modulus and high toughness[6,7,8,9,10,11,12,13,14]. The employment of rare earth oxides (CeO_2 and Sc_2O_3) as zirconia phase stabilizers, and rare-earth zirconates represents a promising solution. To this purpose, the TBCs should preferably have thermal conductivity of about 0.5^{-1} Wm-1K-1, CTE higher than 9×10^{-6} K-1, hardness higher than 500 HV_{300g}. For example, plasma-sprayed CYSZ TBCs have exhibited better phase stability and thermal shock resistance than the YSZ ones as well as better resistance to high-temperature sintering, higher CTE and higher hardness[15,16,17,18,19].

Lanthanum zirconate is another suitable material due to its lower thermal conductivity (1.6 Wm-1K-1 against 2.2 Wm-1K-1 for YSZ, bulk materials; 0.7-0.8 Wm-1K-1 against 0.8-1.2 Wm-1K-1 for coatings)[10,11,20], lower sintering activity, lower Young's modulus and lower ionic conductivity (9.2×10^{-4} $\Omega^{-1}cm^{-1}$ against 0.1 $\Omega^{-1}cm^{-1}$ for YSZ, at 1000 °C), which is expected to reduce oxygen propagation and, consequently, the oxidation of the bond coat surface, which is recognized as one of the main factors affecting the durability of a TBC[21].

These coatings can be employed in multilayered systems, where the TBC is generally composed of an inner coating made of YSZ and the upper coating consists of rare-earth zirconate. Some previous investigations have demonstrated that these systems exhibit better performance under thermal cycling conditions than conventional YSZ systems and, thus, are able to replace the same ones in next-generation turbine engine applications.

In this work, the microstructural and thermal properties of various plasma-sprayed ceramic coatings are investigated in the purpose to develop a novel multilayered system with enhanced performance.

Materials and methods

Plasma spraying

The APS system available at the ENEA Brindisi Research Centre, equipped with a F4-MB plasma torch

(Sulzer Metco, Wolhen, Switzerland) with 6 mm internal diameter nozzle, was employed for TBC deposition. Before plasma spraying, IN738 super-alloy disks (Φ = 25, thickness = 4 mm) were sand-blasted using alumina abrasive powder (Metcolite F, Sulzer Metco, Westbury, NY), in order to increase their surface roughness and to improve the mechanical interlocking between coating and substrate. They were ultrasonically cleaned in ethanol, placed on a rotating sample holder and coated.

The raw materials used for coating fabrication were commercially available powders, known as partially yttria stabilized zirconia (YSZ, ZrO_2-8 wt.% Y_2O_3, Metco 204NS, Sulzer Metco, Westbury, NY, 11-125 µm), ceria-yttria stabilized zirconia (CYSZ, ZrO_2-25 wt.% CeO_2-2.5 wt.% Y_2O_3, Metco 205NS, Sulzer Metco, Westbury, NY, 10-110 µm) and lanthanum zirconate (LZ or $La_2Zr_2O_7$, 43wt.% ZrO_2-57wt.% La_2O_3, Trans-Tech Inc, Adamstown, MD, 37-149 µm). An intermediate 160 µm thick bond coat was previously deposited starting from a powder with 52Ni-10Co-23Cr-12Al-3Re (wt.%) chemical composition and particle size distribution in the nominal range between 37 and 44 µm.

For characterization purposes, the ceramic TBCs were deposited with a final thickness of 2 mm. The spraying parameters used in this work are summarized in Table

	YSZ	CYSZ	$La_2Zr_2O_7$
Current [A]	600	600	500
Voltage [V]	64	70	60
Turntable speed [rpm]	100	100	100
Substrate tangential speed [mm/s]	2083	2083	2083
Gun velocity [mm/s]	4	4	4
Primary gas Ar flow rate [slpm]	33	38	35
Secondary gas H_2 flow rate [slpm]	10	11	8
Stand-off distance [mm]	100	120	100
Carrier gas Ar flow rate [slpm]	2.6	2.6	2.6
Powder feed rate [g/min]	42.6	44	34
Injector diameter [mm]	1.8	1.8	1.8
Injector angle [°]	90	90	90
Distance torch-injector [mm]	6	6	6

TABLE 1 Plasma spraying parameters used in this work (slpm – standard litres per minute)

1. An air cooling jet (pressure = 5 bar) was used to reduce the temperature of the substrates during processing. Multilayered systems have also been fabricated. The substrates were coated with the same bond coat, a first 200 µm thick CYSZ or YSZ layer and one or more ceramic further top coats, made of rare earth zirconates with a total thickness between 200 and 550 µm.

Characterization

Phase composition of as-sprayed coatings was investigated using an X-ray Powder Diffractometer (PW1880, Philips, Almelo, The Netherlands) operating with CuKα radiation, produced at 40 kV and 40 mA. The θ-2θ scan was performed between 20 and 80° by step width of 0.02°. The time per step was set to 5 s.

The cross sections of plasma-sprayed coatings were cut by low speed diamond saw, cold mounted in vacuum in polymer and polished to 0.25 µm. Then they were analyzed by scanning electron microscopy (SEM-LEO 438 VP, Carl Zeiss AG, Oberkochen, Germany).

For quantitative microstructural measurements, the SEM images were processed by free-domain image analysis software (Image J, U.S. National Institutes of Health, Bethesda, MD).

Free-standing coatings for thermal characterization were cut and stripped off from the substrates by chemical etching, by using a 50/50 (vol.%) HCl-H_2O solution, and cleaned. Some coatings were heated at 6 °C/min to 1315 °C, and annealed in air atmosphere up to 50 h. The linear thermal expansion was measured using a Netzsch dilatometer (TMA 402, Netzsch-Geratebäu GmbH, Selb, Germany) in static air atmosphere. The thermal expansion measurements were carried out in static air on free-standing coatings (sample length = 7 mm), from room temperature up to 900 °C at heating rate of 10 °C/min. Three consecutive scans were collected for each type of samples and both in-plane and out-of-plane thermal expansions were measured.

Specific heat measurements were performed between room temperature and 1250 °C using a simultaneous thermal analyzer (Model STA 429, Netzsch-Geratebäu GmbH, Selb, Germany), equipped with a sample holder for differential scanning calorimetry (DSC), following the procedure described in [15].

The measurements were carried out in static air on ap-

proximately 3 mm x 3 mm x 2 mm sized samples. The sample weight used for CP measurement was approximately 120 mg. On each sample the effect of the first heating cycle on specific heat capacity was investigated. Then three consecutive measurement cycles were considered to calculate an average value: the measurements were performed between room temperature and 1250 °C at heating rate of 10 °C/min. The ratio method using a synthetic sapphire (0.775 J/g K – NBS literature value) as calibrant was used to determine the specific heat curves of TBCs [22].

Results and discussion

Phase stability

XRD analyses were performed on as-sprayed and annealed coatings. According to detailed investigation reported in previous paper, as-sprayed YSZ coatings are mainly composed of t' tetragonal zirconia phase, but after 50 h of exposure at 1315 °C they partially decompose [16], so that the final coatings are composed of high-yttria tetragonal, high-yttria cubic, low-yttria tetragonal and monoclinic zirconia phases.

On the contrary, CYSZ coatings exhibit better phase stability, due to the absence of monoclinic phase after thermal aging [15].

The same measurements have been performed on $La_2Zr_2O_7$ coatings and are not herein reported for sake of brevity. These coatings are composed of a single

YSZ	CYSZ	$La_2Zr_2O_7$
12.2 ± 1.6	10.2 ± 2.0	9.1 ± 0.5

TABLE 2 Porosity values for the ceramic coatings herein employed

cubic pyrochlore phase and show no phase transition after thermal aging at 1315 °C, but only a decrease in the width of the peaks, which are broad in as-sprayed condition due to the small crystallite size and crystalline disorder. The precipitation of ZrO_2 after annealing could not be appreciated by XRD.

Microstructure

As shown in Figures 1-3, all the ceramic TBCs herein analyzed exhibit a typical splat-like microstructure, composed of overlapped lamellae, approximately parallel to coating/substrate interface, separated by splat boundaries and embedded in a network of microcracks and voids. The thickness of the lamellae is approximately between 1 and 5 μm.

The splat boundaries typically affect heat transfer and thermal conductivity, while the vertical microcracks enhance high-temperature strain tolerance. The former originated during coating build-up due to weak bonding between deposited splats, depending on the velocity of impact of the molten droplets and their solidification rate. In turn, the latter initiated from the splat boundaries as a consequence of stress relaxation during rapid cooling to room temperature. Globular
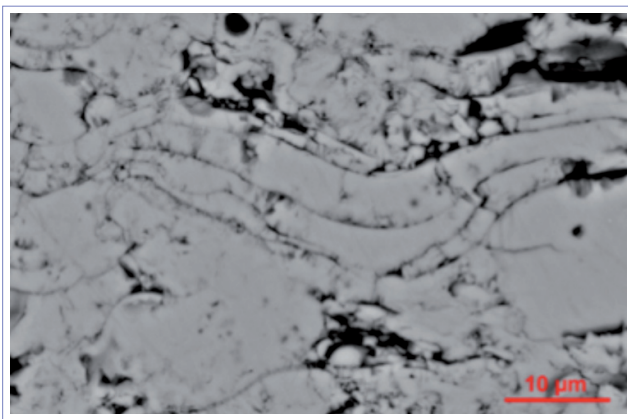

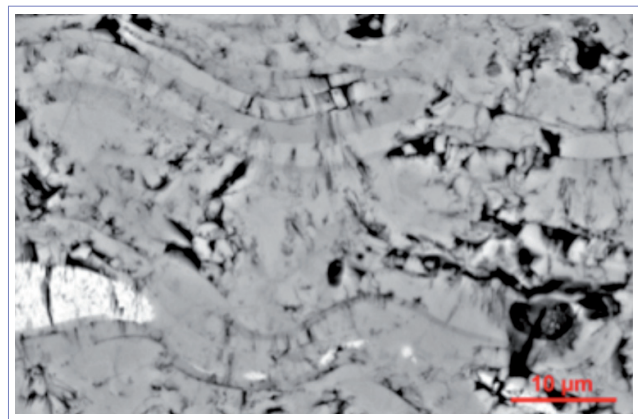**FIGURE 1** Polished cross section of YSZ coating showing a lamellar microstructure

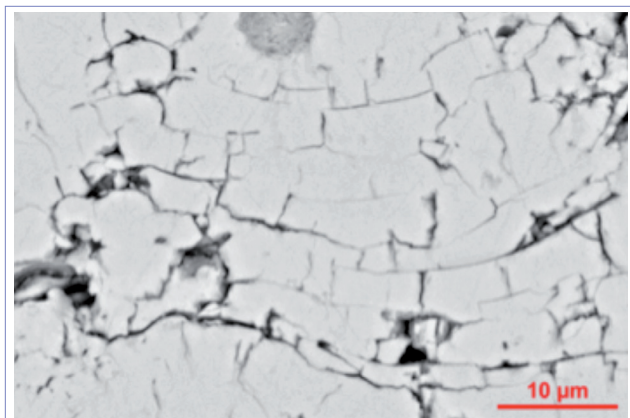**FIGURE 2** Polished cross section of CYSZ coating showing a lamellar microstructure

FIGURE 3 Polished cross section of $La_2Zr_2O_7$ coating showing a lamellar microstructure

T = 50-900 °C	YSZ	CYSZ	$La_2Zr_2O_7$
CTE in-plane [10^{-6} K^{-1}]	10.7	12.6	9.2
CTE out-of-plane [10^{-6} K^{-1}]	10.8	10.1	9.2

TABLE 3 Thermal expansion coefficients for plasma-sprayed coatings

pores derived from imperfect filling during coating build-up and play a significant role on the final thermal and mechanical properties.

As shown in Figure 2, in CYSZ coating different areas with different grey contrast can be noticed. The brighter areas are richer in CeO_2 stabilizer and are then related to the presence of cubic zirconia.

Table 2 reports the porosity values for the ceramic TBCs herein developed. Note that YSZ and CYSZ coatings are more porous than $La_2Zr_2O_7$ ones: this behavior can be explained in terms of different morpho-

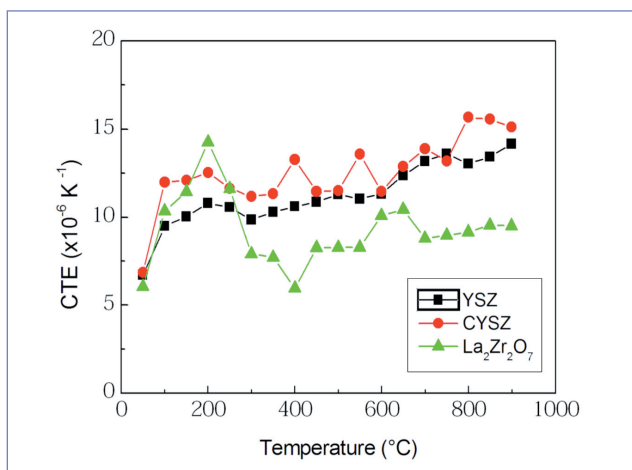logy of the starting powders as well as of different processing parameters.

Thermal properties
The thermal expansion curves of plasma-sprayed coatings were measured in-plane and out-of-plane directions between 50 and 900 °C. The thermal expansion increases linearly over the entire temperature range. The mean values of thermal expansion coefficients for as-sprayed TBCs are given in Table 3. These values are higher than those previously reported for CYSZ, YSZ and LZ coatings[20,23,24].

The CTE is strongly related to the crystal structure and to any phase transitions which can occur during heating. The out-of-plane CTE is affected by interlamellar cracks, while in-plane CTE is affected by vertical cracks. The in-plane CTE is approximately 10.7 x 10^{-6} K^{-1} for as-sprayed YSZ coating, 12.6 x 10^{-6} K^{-1} for CYSZ coatings, and 9.2 x 10^{-6} K^{-1} for $La_2Zr_2O_7$ ones. CYSZ coatings exhibit the highest CTE, due to the presence of the cubic structure in as-sprayed state and higher concentration of oxygen vacancies.

The thermal expansion is one of the most significant parameters in order to predict the lifetime of TBCs. Figure 4 shows in-plane thermal expansion coefficient versus temperature for YSZ, CYSZ and $La_2Zr_2O_7$ coatings. Note that the CTE increases as temperature raises for all the coatings, due to the intensification of the crystal lattice vibration. The CTE of YSZ coatings increases from 6.7 x 10^{-6} K^{-1} to 14.2 x 10^{-6} K^{-1} at 900 °C. It increases from 6.9 x 10^{-6} K^{-1} to 15.1 x 10^{-6} K^{-1} for CYSZ coatings, from 6 x 10^{-6} K^{-1} to 9.5 x 10^{-6} K^{-1} for $La_2Zr_2O_7$ ones.

The increase is more pronounced for YSZ e CYSZ; above 300 °C their CTE is higher than that of $La_2Zr_2O_7$ coating and therefore closer to that of the bond coat, thus suggesting lower thermal stresses at high temperature at the interface between the overlapped layers, and higher resistance to crack propagation. In the whole temperature range investigated no simple dependence of CTE on temperature was

FIGURE 4 Thermal expansion coefficient vs. temperature for different TBCs

detected for $La_2Zr_2O_7$ coatings. A sudden decrease above 200 °C can be noticed, and a further decrease above 650 °C: a similar trend was noticed previously [11]. These peaks can be probably linked to the existence of internal stresses, while phase changes and sintering can be discarded. This behavior can be harmful for practical applications, because the mismatch in CTE values can promote thermal stresses and crack formation during cycling. However, the relatively low CTE and toughness of lanthanum zirconate can be enhanced by chemical doping with heavy atoms with large ion radii.

Figure 5 shows the specific heat capacity of plasma-sprayed coatings during the first heating cycle. The specific heat capacity of YSZ coating is 0.45 $Jg^{-1}K^{-1}$ at 100 °C and 0.37 $Jg^{-1}K^{-1}$ at 1150 °C; for CYSZ it is 0.57 $Jg^{-1}K^{-1}$ at 100 °C and 0.80 $Jg-1K^{-1}$ at 1150 °C, for $La_2Zr_2O_7$ it is 0.37 $Jg^{-1}K^{-1}$ at 100 °C and 0.42 $Jg^{-1}K^{-1}$ at 1100 °C. Therefore, lanthanum zirconate coatings show the lowest specific heat capacity at room temperature, while at the maximum temperature YSZ coatings are characterized by the lowest CP. The first heating cycle on as-sprayed coatings typically promotes irreversible changes, such as first-stage sintering and stress relaxation and thus a corresponding increase in specific heat capacity at high temperature, whereas no deviations are observed in the next runs. Changes at crystal lattice scale may also affect the C_P values. The sintering of the porous microstruc-

ture generally occurs at T > 1200 °C, due to the closure of fine pores and microcracks. It is well established that the sintering necks reduce the space between the lamellae and close the vertical microcracks, thus reducing the thermal insulation and the structural elasticity. The specific heat average curves of as-sprayed coatings are plotted in Figure 6 as a function of temperature: C_P (T) curves were calculated as a mean value of three consecutive measurement cycles. The specific heat capacity for YSZ is 0.49 $Jg^{-1}K^{-1}$ at 100 °C and 0.51 $Jg^{-1}K^{-1}$ at 1150 °C, for CYSZ it is 0.44 $Jg^{-1}K^{-1}$ at 100 °C and 0.71 $Jg^{-1}K^{-1}$ at 1150 °C, whereas for $La_2Zr_2O_7$ it is 0.52 $Jg^{-1}K^{-1}$ at 100 °C and 0.6 $Jg^{-1}K^{-1}$ at 1100 °C.

With respect to the first heating cycle the specific heat capacity increases for YSZ and $La_2Zr_2O_7$ coatings, whereas it decreases for CYSZ coatings, thus suggesting a better resistance to high-temperature changes. In addition, prolonged exposure at 1315 °C promotes a further increase in the specific heat capacity for YSZ coatings, while a decrease is noticed for CYSZ coatings [15,16].

Multilayered ceramic TBCs

The single TBC systems herein employed exhibit satisfactory performance for current turbine applications; however, in the next-generation turbine engines further increases in thrust-to-weight ratio and higher gas inlet temperature are expected. This involves higher tempe-
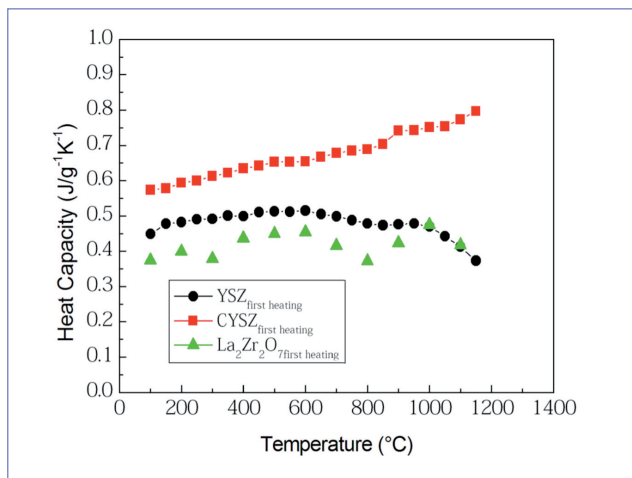

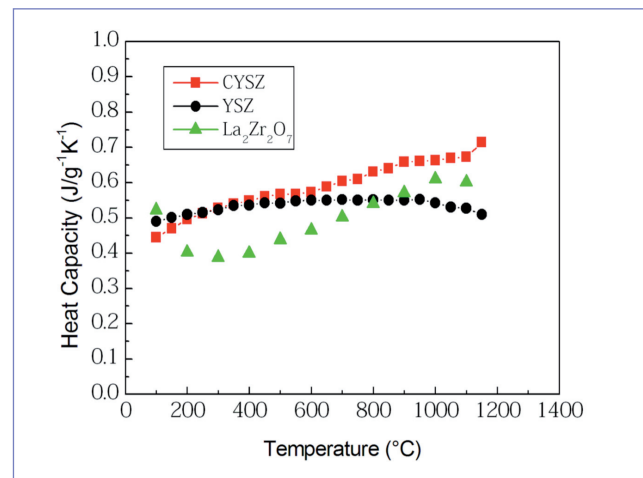**FIGURE 5** Specific heat capacity of plasma-sprayed ceramic coatings during the first heating cycle

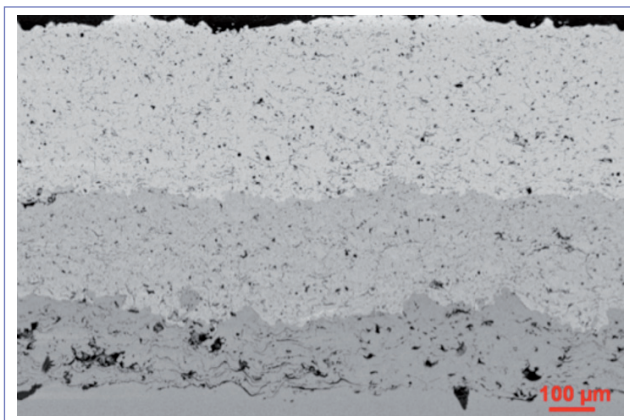**FIGURE 6** Specific heat capacity of plasma-sprayed ceramic coatings

FIGURE 7 Multilayered thermal barrier coating, composed of substrate (at the bottom), MCrAlY bond coat, intermediate CYSZ layer and upper $La_2Zr_2O_7$ top coat

rature capability and better protection against the environmental attack of corrosive media as calcium magnesium alumino-silicate (CMAS) and erosive agents. Therefore, the search for low-conductivity ceramic materials needs to be supported by an optimization of TBC architecture as well as by enhancements in powder manufacturing and thermal spray processing[25].

From this point of view, multilayered TBCs have been properly designed in order to overcome the limitations of single layer TBCs. These systems are able to increase the operating temperature and to better accommodate the thermal stresses arising from thermal expansion mismatch between bond coat and top coat and the diffusion of oxygen, which typically assists the formation and the growth of the TGO (thermally grown oxide) at top coat/bond coat interface and then the TBC spallation. These systems are composed of two or more ceramic layers and YSZ is commonly applied as an intermediate coating and environmentally protected by an upper coating with higher temperature capability.

Double APS TBCs, composed of an inner YSZ layer and an upper $La_2Zr_2O_7$ layer, exhibited enhanced durability during thermal cycling tests at different surface temperatures (1250, 1350 and 1450 °C). At the lowest temperature the double system showed thermal cyclic performance (more than 4000 cycles) better than that of single $La_2Zr_2O_7$ layer (137-977 cycles) and comparable to that of single YSZ layer. At about 1350 °C dou-

ble layer system exhibited better cyclic lifetime (1000-2346 cycles) than those of single YSZ and double YSZ/$Nd_2Zr_2O_7$ TBC systems (220-1000 and 1748 cycles, respectively)[26,27]. YSZ/$La_2Zr_2O_7$ TBC survived more than 1200 cycles at 1450 °C, showing better temperature capability than YSZ one. At 1250 °C the lifetime of double YSZ/$SrZrO_3$ TBC was two times higher than that of YSZ one, while at temperatures higher than 1300 °C these systems possessed the same durability[27].

An advanced multilayered TBC system has then been developed in order to increase the high-temperature performance of single layer systems. This system has been recently patented at ENEA by Di Girolamo et al. as *"Rivestimento protettivo per componenti realizzati in superlega"*, Italian Patent n. BO2012A000577.

Figure 7 shows the cross section of a multilayered TBC, composed of a metal substrate (on the bottom), a metal bond coat, an intermediate CYSZ layer and an upper $La_2Zr_2O_7$ layer.

The porosity of CYSZ coating can be chosen between 8 and 15%, while the porosity of the $La_2Zr_2O_7$ layer can be set between 4 and 12%, depending on the expected operating conditions. Their hardness has to be higher than 500 HV_{300g}. Moreover, the CTE of the intermediate CYSZ coating is higher than 12 x 10^{-6} K^{-1}, while the CTE of zirconate layers is of about 9 x 10^{-6} K^{-1}. The CYSZ coating is able to substitute the standard YSZ coating, due to its higher phase stability, CTE, hardness and resistance to high-temperature sintering. Alternatively, the multilayered system can be composed of two or more ceramic top coats whose CTE and porosity gradually decrease from the bottom to the top surface. To the aim rare-earth zirconates, such as $Nd_2Zr_2O_7$, $Sm_2Zr_2O_7$, $Gd_2Zr_2O_7$ and $SrZrO_3$, can be successfully employed.

Conclusions

Different ceramic powders were air plasma sprayed to produce TBCs for turbine engine applications. All the coatings showed a lamellar microstructure with typical defects, such as pores, microcracks and splat boundaries, which tended to disappear after high-temperature exposure due to sintering phenomena. CYSZ and $La_2Zr_2O_7$ coatings exhibited enhanced phase stability above 1300 °C, in comparison with YSZ ones.

CYSZ coatings exhibited the highest in-plane CTE, followed by YSZ and $La_2Zr_2O_7$ coatings.

The specific heat capacity was affected by sintering phenomena during measurement cycles: it tended to increase for YSZ and $La_2Zr_2O_7$ TBCs, while it decreased for CYSZ ones. A multilayered TBC system was finally developed. In this system the ceramic top coat is composed of two or more ceramic layers, a first layer made of CYSZ and one or more rare-earth zirconate layers, in order to overcome the current limits of conventional TBC systems, especially looking at much severe applications, at temperature higher than 1300 °C, in presence of corrosive media and when high thermal stresses are expected due to long-term thermal cycling. This system was patented at ENEA by Di Girolamo et al. ●

Acknowledgments

references

[1] National Research Council. *Coatings for High-temperature structural materials: trends and opportunities.* National Academy of Sciences. Washington (1996).

[2] X.Q. Cao, R. Vassen, D. Stover (2004), *"Ceramic materials for thermal barrier coatings"*, J. Eur. Ceram. Soc., 24, 1-10.

[3] X. Chen, M.Y. He, I.T. Spitsberg, N.A. Fleck, J.W. Hutchinson, A.G. Evans (2004), *"Mechanisms governing the high temperature erosion of thermal barrier coatings"*, Wear, 256, 735-746.

[4] M.P. Borom, C.A. Johnson, L.A. Peluso (1996), *"Role of environmental deposits and operating surface temperature in spallation of air plasma sprayed thermal barrier coatings"*, Surf. Coat. Technol., 86/87, 116-126.

[5] B.R. Marple, J. Voyer, C. Moreau, D.R. Nagy (2000), *"Corrosion of thermal barrier coatings by vanadium and sulfur compounds"*, Mater. High Temp., 17, 397-412.

[6] S.A. Tsipas (2010), *"Effects of dopants on the phase stability of zirconia-based plasma sprayed thermal barrier coatings"*, J. Eur. Ceram. Soc., 30, 61-72.

[7] N. Curry, N. Markocsan, X.A. Li, A. Tricoire, M. Dorfman (2011), *"Next generation thermal barrier coatings for the gas turbine industry"*, J. Therm. Spray Technol., 20, 108-115.

[8] H. Dai, J. Li, X. Cao, J. Meng (2009), *"Thermal barrier coating material"*, US20097597971.

[9] J. Wu, X. Wei, N.P. Padture, P.G. Klemens, M. Gell, E. Garcia et al. (2002), *"Low-thermal-conductivity rare-earth zirconates for potential thermal-barrier-coating applications"*, J. Am. Ceram. Soc., 85, 3031-3025.

[10] R. Vassen, X. Cao, F. Tietz, D. Basu, D. Stover (2000), *"Zirconates as new materials for thermal barrier coatings"*, J. Am. Ceram. Soc., 83, 2023-2028.

[11] H. Chen, Y. Gao, S. Tao, Y. Liu, H. Luo (2009), *"Thermophysical properties of lanthanum zirconate coating prepared by plasma spraying and the influence of post-annealing"*, J. Alloys Comp., 486, 391-399.

[12] D. Stover, G. Pratch, H. Lehmann, M. Dietrich, J. E. Doring, R. Vassen (2004), *"New materials concepts for the next generation of plasma-sprayed thermal barrier coatings"*, J. Therm. Spray Technol.,13, 76-83.

[13] J. Hu, H. Zhao, S. Tao, X. Zhou, C. Ding (2010), *"Thermal conductivity of plasma sprayed $Sm_2Zr_2O_7$ coating"*, J. Eur. Ceram. Soc., 30, 799-804.

[14] Y. Wang, H. Guo, S. Gong (2009), *"Thermal physical properties and thermal shock resistance of $La_2Ce_2O_7$ thermal barrier coatings with segmented structure"*, Ceram. Int., 35, 2639-2644.

[15] G. Di Girolamo, C. Blasi, M. Schioppa, L. Tapfer (2010), *"Structure and thermal properties of heat treated plasma sprayed ceria-yttria co-stabilized zirconia coatings"*, Ceram. Int., 36, 961-968.

[16] G. Di Girolamo. C. Blasi, L. Pagnotta, M. Schioppa (2010), *"Phase evolution and thermophysical properties of plasma sprayed thick zirconia coatings after annealing"*, Ceram. Int., 36, 2273-2280.

[17] S.Y. Park, J.H. Kim, M.C. Kim, H.S. Song, C.G. Park (2005), *"Microscopic observation of degradation behaviour in yttria and ceria stabilized zirconia thermal barrier coatings under hot corrosion"*, Surf. Coat. Technol., 190, 357-365.

[18] M. Alfano, G. Di Girolamo, L. Pagnotta, D. Sun, J. Zekonyte, R.J.K. Wood (2010), *"The influence of high-temperature sintering on microstructure and mechanical properties of free-standing APS CeO_2-Y_2O_3-ZrO_2 coatings"*, J. Mater. Sci., 45, 2662-2669.

[19] M. Alfano, G. Di Girolamo, L. Pagnotta, D. Sun (2010), *"Processing, microstructure and mechanical properties of air plasma-sprayed ceria-yttria co-stabilized zirconia coatings"*, Strain, 46, 409-418.

[20] H. Zhou, D. Yi, Z. Yu, L. Xiao (2007), *"Preparation and thermophysical properties of CeO_2 doped $La_2Zr_2O_7$ ceramic for thermal barrier coatings"*, J. Alloys Comp., 438, 217-221..

[21] A.G. Evans, D.R. Mumm, J.W. Hutchinson, G.H. Meier, F.S. Petit (2001), *"Mechanisms controlling the durability of thermal barrier coatings"*, Prog. Mater. Sci., 46, 505-553.

[22] J. B. Henderson, W. D. Emmerich, E. Wassmer (1988), *"Measurement of the specific heat and heat of decomposition of a polymer composite to high temperatures"*, J. Therm. Anal., 33 (4), 1067-1077.

[23] S. Ahmaniemi, P. Vuoristo, T. Mantyla, F. Cernuschi, L. Lorenzoni (2004), *"Modified thick thermal barrier coatings: thermophysical characterization"*, J. Eur. Ceram. Soc., 24, 2669-2679.

[24] W. Ma, D.E. Mack, R. Vassen, D. Stover (2008), *"Perovskite-type strontium zirconate as a new material for thermal barrier coatings"*, J. Am. Ceram. Soc., 91, 2630-2635.

[25] G. Di Girolamo, L. Pagnotta (2011), *"Thermally sprayed coatings for high-temperature applications"*, Recent Patents on Mater. Sci., 4, 173-190.

[26] U. Bast, E. Schumann (2002), *"Development of novel oxide materials for TBCs"*, Ceram. Eng. Sci Proc., 23, 525-532.

[27] R. Vassen, F. Traeger, D. Stover (2004), *"New thermal barrier coatings based on pyrochlore/YSZ double-layer systems"*, Int. J. Appl. Ceram. Technol., 1, 351-361.